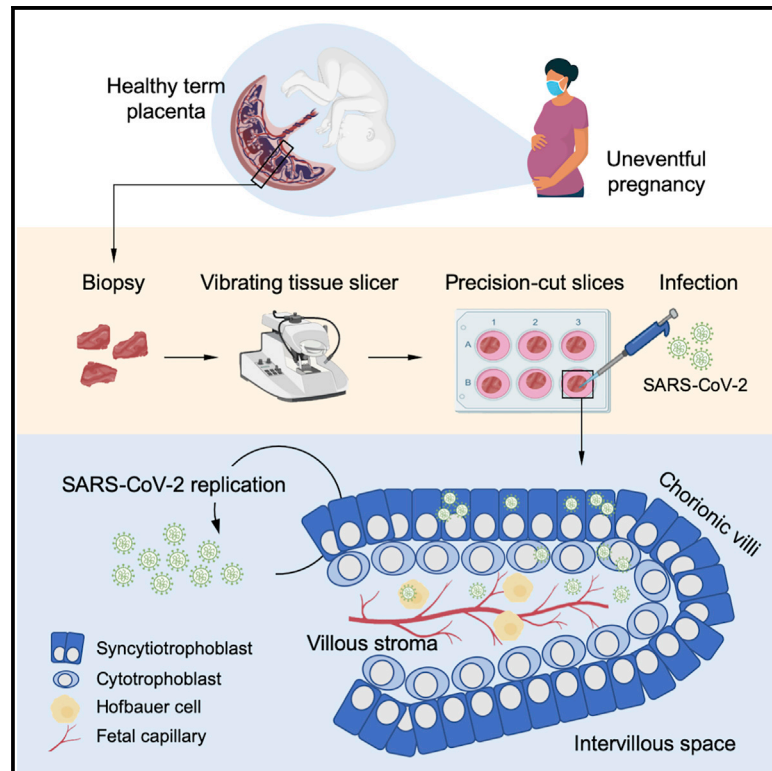Report

SARS-CoV-2 can infect and propagate in human placenta explants

Graphical abstract

Authors

Amal Fahmi, Melanie Brügger,
Thomas Démoulins, ..., Volker Thiel,
David Baud, Marco P. Alves

Correspondence

david.baud@chuv.ch (D.B.),
marco.alves@vetsuisse.unibe.ch (M.P.A.)

In brief

Fahmi et al. use precision-cut slices of human placental tissue to study SARS-CoV-2 infection at the maternal-fetal interface. They demonstrate that SARS-CoV-2 infects several cellular compartments and propagates in human placenta. In addition, the authors find a significant association between placental ACE2 expression levels and the release of infectious SARS-CoV-2.

Highlights

- *Ex vivo* modeling of SARS-CoV-2 infection at the maternal-fetal interface in human

- SARS-CoV-2 replicates and propagates in human placenta

- Magnitude of infectious SARS-CoV-2 release is related to ACE2 expression

- SARS-CoV-2 proteins and/or RNA are detected in different placental cells

CellPress

Report

SARS-CoV-2 can infect and propagate in human placenta explants

Amal Fahmi,[1,2,3,7] Melanie Brügger,[1,2,7] Thomas Démoulins,[1,2,7] Beatrice Zumkehr,[1,2] Blandina I. Oliveira Esteves,[1,2] Lisamaria Bracher,[1,2] Carlos Wotzkow,[4] Fabian Blank,[4,5] Volker Thiel,[1,2] David Baud,[6,7,*] and Marco P. Alves[1,2,7,8,*]

[1]Institute of Virology and Immunology, Bern, Switzerland
[2]Department of Infectious Diseases and Pathobiology, Vetsuisse Faculty, University of Bern, Bern, Switzerland
[3]Graduate School for Cellular and Biomedical Sciences, University of Bern, Bern, Switzerland
[4]Department for BioMedical Research (DBMR), University of Bern, Bern, Switzerland
[5]Department of Pulmonary Medicine, Inselspital, Bern University Hospital, Bern, Switzerland
[6]Materno-Fetal and Obstetrics Research Unit, Department "Femme-Mere-Enfant," Lausanne University Hospital, Lausanne, Switzerland
[7]These authors contributed equally
[8]Lead contact
*Correspondence: david.baud@chuv.ch (D.B.), marco.alves@vetsuisse.unibe.ch (M.P.A.)
https://doi.org/10.1016/j.xcrm.2021.100456

SUMMARY

The ongoing SARS-CoV-2 pandemic continues to lead to high morbidity and mortality. During pregnancy, severe maternal and neonatal outcomes and placental pathological changes have been described. We evaluate SARS-CoV-2 infection at the maternal-fetal interface using precision-cut slices (PCSs) of human placenta. Remarkably, exposure of placenta PCSs to SARS-CoV-2 leads to a full replication cycle with infectious virus release. Moreover, the susceptibility of placental tissue to SARS-CoV-2 replication relates to the expression levels of ACE2. Viral proteins and/or viral RNA are detected in syncytiotrophoblasts, cytotrophoblasts, villous stroma, and possibly Hofbauer cells. While SARS-CoV-2 infection of placenta PCSs does not cause a detectable cytotoxicity or a pro-inflammatory cytokine response, an upregulation of one order of magnitude of interferon type III transcripts is measured. In conclusion, our data demonstrate the capacity of SARS-CoV-2 to infect and propagate in human placenta and constitute a basis for further investigation of SARS-CoV-2 biology at the maternal-fetal interface.

INTRODUCTION

The ongoing coronavirus disease 2019 (COVID-19) pandemic is caused by infection with severe acute respiratory syndrome-coronavirus 2 (SARS-CoV-2), a betacoronavirus with major similarities to SARS-CoV, the causative pathogen of SARS. The cell surface receptor for both viruses, the angiotensin-converting enzyme 2 (ACE2), is highly expressed by epithelial cells of the upper and lower respiratory tract.[1] In addition, SARS-CoV and SARS-CoV-2 both use the endogenous plasma membrane serine protease transmembrane serine protease 2 (TMPRSS2) as a factor for priming and activation. Interestingly, the expression of ACE2 and TMPRSS2 are not restricted to the lung tissue but are also expressed in cardiomyocytes, enterocytes, endothelial cells, and placental trophoblasts, indicating that SARS-CoV-2 may have a wide cellular tropism.[2–6] Several extrapulmonary complications are described, including acute cardiac and kidney injury, neurological and gastrointestinal manifestations, endothelial damage, and thrombosis in various organs.[7,8]

There is epidemiologic evidence that pregnant women have an elevated risk of developing severe COVID-19 in comparison to age-matched non-pregnant women.[9–11] Also, up to 40% of SARS-CoV-2 infections during pregnancy are associated with adverse outcomes such as prematurity, miscarriage, preeclampsia, and stillbirth.[5,12–14] Large cohort studies have shown that preterm birth, stillbirth, and preeclampsia were significantly increased.[15] Furthermore, there are indications from several case reports that SARS-CoV-2 infection during pregnancy is associated with placental pathological changes, including placentitis, intervillositis, fibrin deposition, and decidual vascular injury.[14,16–19] Moreover, placental infection was reported with the presence of the viral RNA in the umbilical cord, the placental villi, fetal membranes, and trophoblasts, raising concerns that SARS-CoV-2 could affect fetal development.[20,21] Severe neonatal COVID-19 is described and sporadic cases of vertical transmission were reported.[22–26]

Assuming the critical nourishing and protecting functions of the placenta, it is crucial to evaluate in further detail the impact of SARS-CoV-2 infection during pregnancy. However, due to the high degree of interspecies placenta diversity, animal models of human placenta diseases are of limited relevance.[27] To recapitulate human biology at the maternal-fetal interface, we used an *ex vivo* model based on organotypic cultures of precision-cut slices (PCSs) of human placenta and evaluated the permissiveness and tropism of third-trimester placenta to SARS-CoV-2.
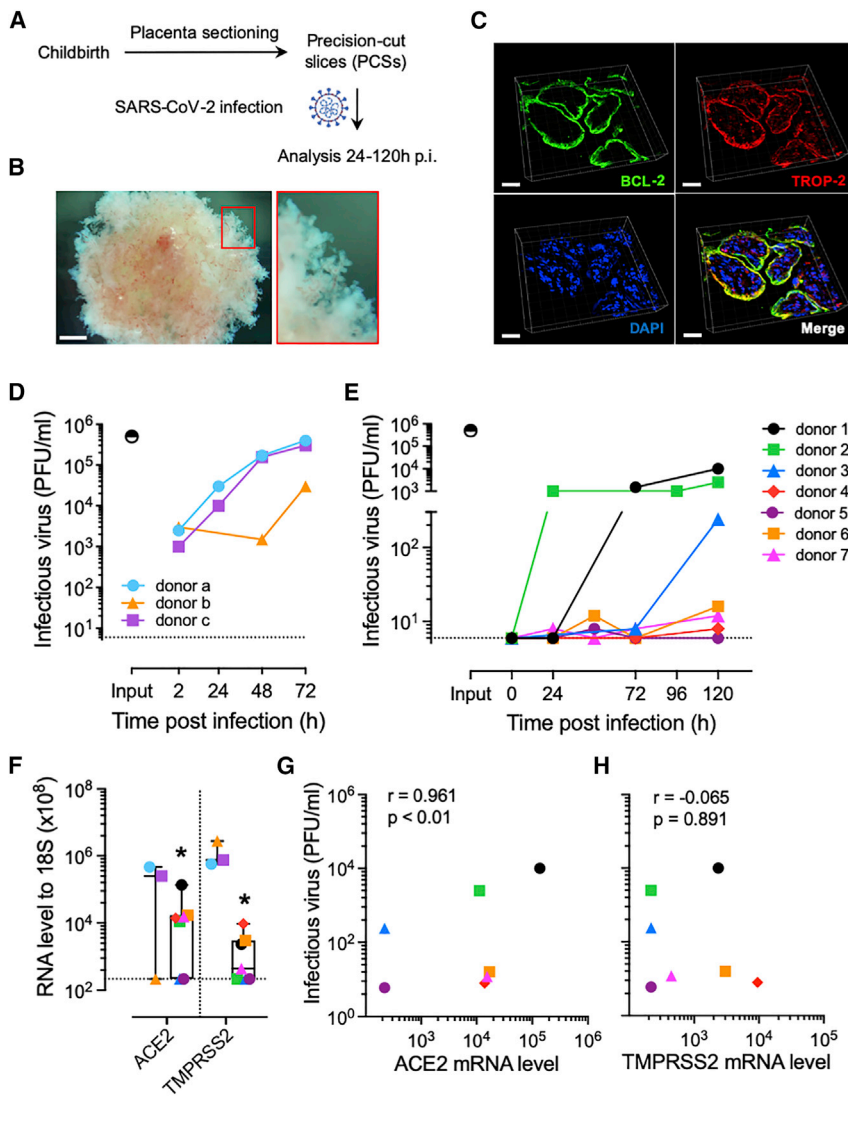
Figure 1. SARS-CoV-2 is propagating in human placenta PCSs

(A) Placenta PCSs were prepared as slices of 500–700 μm and challenged with SARS-CoV-2 at a rate of 5×10^5 PFU per slice and analyzed 24–120 h p.i.

(B) Representative stereomicroscopic image showing a preserved villous microstructure of placenta PCSs after 120 h of culture. Scale bar, 500 μm.

(C) Representative 3D rendering micrograph of the syncytiotrophoblast (BLC-2, green) and trophoblast (TROP-2, red) layers in placenta PCS cultures. DAPI (blue). Scale bar, 30 μm.

(D) WD-NECs were infected apically with 5×10^4 PFU per insert. The infectious virus release was evaluated in apical washes 24 to 72 h p.i. Each symbol represents an individual donor (n = 3). The input indicates the virus titer adjusted to the volume of inoculum and the horizontal dashed line indicates the baseline measured in mock controls and defined as the detection limit of the PFU assay.

(E) Shedding of infectious virus over time by placenta PCSs exposed to 5×10^5 PFU of SARS-CoV-2. Each symbol represents an individual donor (n = 7). The input indicates the virus titer adjusted to the volume of inoculum and the horizontal dashed line indicates the baseline in mock controls and defined as the detection limit of the PFU assay.
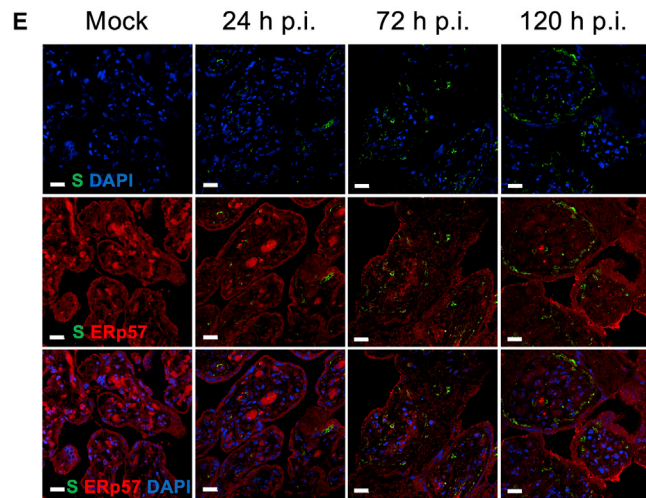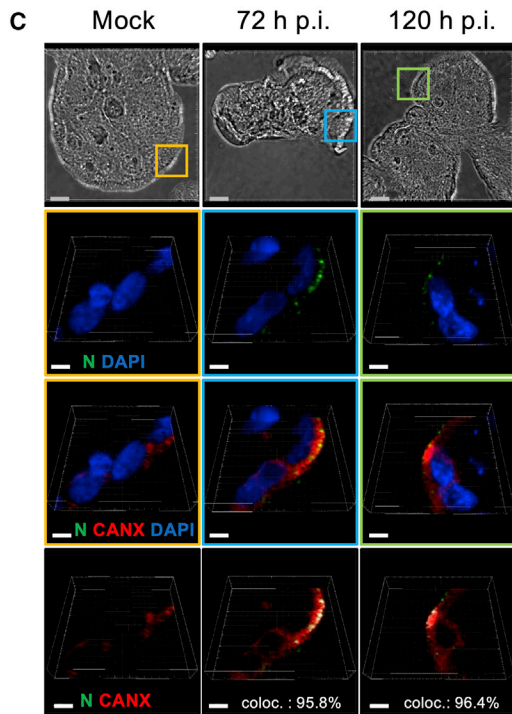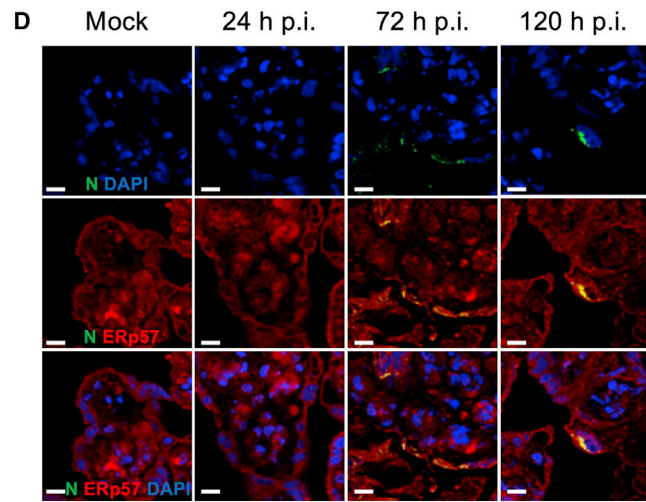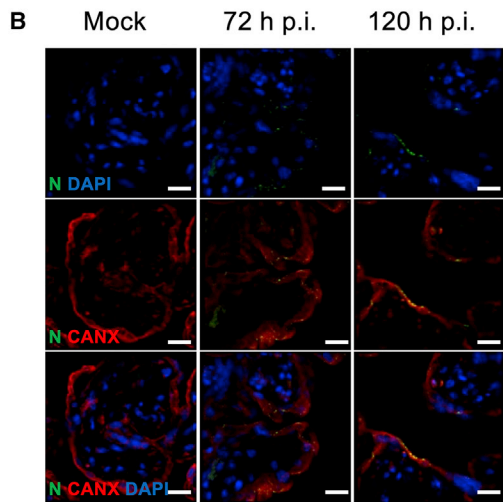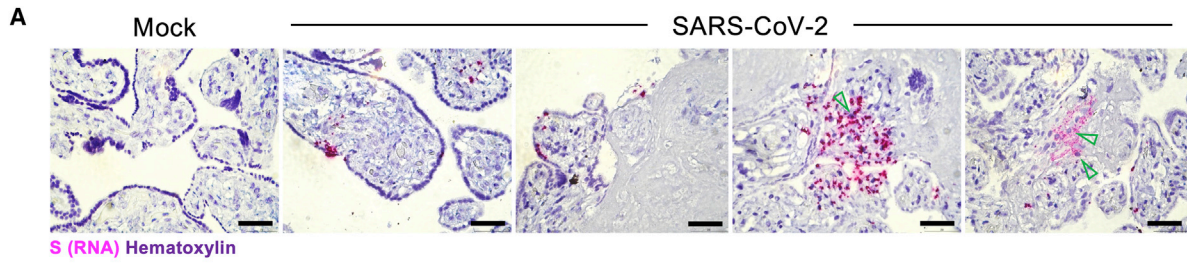
(F) ACE2 and TMPRSS2 mRNA expression levels in non-infected WD-NECs and placenta PCS cultures. Boxplots indicate the median value (centerline) and interquartile ranges (box edges), with whiskers extending to the lowest and the highest values. Each symbol represents an individual donor (n = 3 and n = 7, respectively).

(G and H) Correlation of SARS-CoV-2 titers 120 h p.i. of placenta PCSs and ACE2 (G) and TMPRSS2 (H) mRNA levels. Associations were tested using the Spearman rank correlation test. Each symbol represents an individual donor (n = 7).

RESULTS

Following childbirth, placenta PCSs with a thickness of 500 to 700 μm were prepared and exposed to SARS-CoV-2 or mock treated and analyzed 24–120 h post-infection (p.i.) (Figure 1A). The stereomicroscopic picture in Figure 1B indicates that villous and microstructure in placenta PCSs were preserved following culture over a prolonged period (Figure 1B). To further characterize placenta PCS cultures, we used B cell lymphoma 2 (BCL-2) and trophoblast cell-surface antigen 2 (TROP-2), to visualize syncytiotrophoblasts and cytotrophoblasts, respectively.[28,29] We detected a sharp BCL-2 signal at the surface of the villi with partial overlap with TROP-2, the latter also being detected in the stroma of the villi (Figure 1C). To study the biology of SARS-CoV-2 in human placenta, we exposed PCS cultures to the virus and collected cell culture media and tissue at selected times p.i. As a positive control, we used a surrogate model of the nasal epithelium, well-differentiated primary human nasal epithelial cells (WD-NECs) cultured at the air-liquid interface (ALI). As expected, following infection of WD-NECs with SARS-CoV-2, we observed an exponential increase in infectious virus in apical washes as assessed with a plaque-forming unit (PFU) assay (Figure 1D). Upon infection of placenta PCSs with SARS-CoV-2, we detected an increase in infectious virus release over time in six of seven donors tested, demonstrating that SARS-CoV-2 is propagating in human placenta (Figure 1E). Notably, 50% of susceptible donors led to high levels of infectious virus release, while the others led to rather modest levels. This observation prompted us to determine whether the high variability observed between placenta PCSs donors could be related to ACE2 and/or TMPRSS2 expression. Thus, we measured their mRNA level in non-infected placenta PCSs in comparison to WD-NECs. In line with the robust replication kinetics of SARS-CoV-2 in WD-NECs, we measured significantly lower levels of both molecules in placenta PCSs in comparison to WD-NECs (p < 0.05; Figure 1F). Furthermore, when placental

A Mock — SARS-CoV-2 —

S (RNA) Hematoxylin

B Mock 72 h p.i. 120 h p.i.

N DAPI

N CANX

N CANX DAPI

D Mock 24 h p.i. 72 h p.i. 120 h p.i.

N DAPI

N ERp57

N ERp57 DAPI

C Mock 72 h p.i. 120 h p.i.

N DAPI

N CANX DAPI

N CANX coloc. : 95.8% coloc.: 96.4%

E Mock 24 h p.i. 72 h p.i. 120 h p.i.

S DAPI

S ERp57

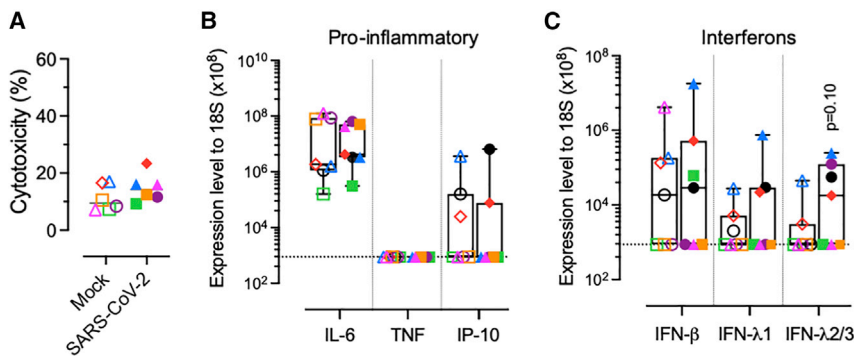S ERp57 DAPI

(legend on next page)

Figure 3. Human placenta PCS responses following SARS-CoV-2 infection

(A) LDH release in placenta PCSs exposed to 5×10^5 PFU of SARS-CoV-2 120 h p.i. Each symbol represents an individual donor (n = 6).

(B and C) Induction of pro-inflammatory cytokines (interleukin-6 [IL-6], tumor necrosis factor [TNF], and interferon [IFN]-γ-induced protein 10 kDa/C-X-C motif chemokine ligand 10 [IP-10/CXCL10]) (B), and (C) IFN (β, λs) transcripts in placenta PCSs 120 h p.i. with mock (empty symbols) or 5×10^5 PFU of SARS-CoV-2 (solid symbols). Boxplots indicate the median value (centerline) and interquartile ranges (box edges), with whiskers extending to the lowest and the highest values. Each symbol represents an individual donor (n = 7). A 2-sided unpaired t test was applied to compare infected to mock control groups.

ACE2 and TMPRSS2 mRNA levels were plotted as a function of infectious virus release, a significant positive association was found for ACE2, suggesting that the susceptibility of human placenta to SARS-CoV-2 infection is related to the expression level of ACE2 (p < 0.01; Figures 1G and 1H).

The infection of human placenta by SARS-CoV-2 is further demonstrated by the detection of the Spike (S) glycoprotein RNA using an *in situ* hybridization approach. The signal was detected in the cell layer at the surface of the villi, indicating infection of syncytiotrophoblasts, but also sporadically underneath the syncytiotrophoblast, suggesting infection of cytotrophoblasts. Furthermore, we observed the presence of the viral S protein RNA in the stroma of the villi, indicating the potential infection of mesenchymal cells. Within the stroma, we also observed S RNA+ cells with a morphology compatible with Hofbauer cells (Figure 2A). To confirm further the SARS-CoV-2 replication in human placenta, we analyzed the subcellular localization of the nucleocapsid (N) protein, a structural glycoprotein of SARS-CoV-2, which is central to the packaging and protection of viral genome and part of the coronavirus replication complex.[30] Notably, these mechanisms take place within the endoplasmic reticulum (ER) and the Golgi compartments.[31] We selected calnexin (CANX), a molecular chaperone of the ER, involved in the maturation of structural viral glycoproteins of numerous viruses.[32] The SARS-CoV-2 N protein signal was localized in the outer layer of the villi corresponding to the syncytiotrophoblast and occasionally in the core of the villi. Contrary to mock-infected control tissue, the two-dimensional (2D)

rendering micrographs show the dotted pattern of the SARS-CoV-2 N protein detectable 72–120 h p.i. (Figure 2B). Next, we investigated the potential interaction between SARS-CoV-2 N protein and CANX. The magnified 3D rendering micrographs presented in Figure 2C demonstrate the perinuclear localization of SARS-CoV-2 N protein in syncytiotrophoblasts. By calculating co-localization percentages, we found a tight relation between CANX and SARS-CoV-2 N protein signals (co-localization index of 95.8% and 96.4%, at 72 and 120 h p.i., respectively; Figure 2C, lower panel). To validate the co-localization, we conducted additional experiments using the ER chaperone ERp57 (also known as glucose-regulated protein, 58 kDa [GRP58]).[33] Similar to CANX, we observed co-localization of the N protein and ERp57 at the level of syncytiotrophoblasts and occasionally in the villi stroma (Figures 3D). We performed a complementary approach with S protein and detected an increase in the signal over time p.i., indicating the replication of SARS-CoV-2. Remarkably, we did not detect co-localization of S protein and ERp57 in any of the donors tested, pointing to distinct maturation mechanisms used by N and S proteins in the placenta secretory pathway (Figure 2E).

Finally, we aimed to evaluate the virus-induced cytotoxicity, inflammatory, and interferon (IFN) type I and III responses following the infection of placenta PCSs. SARS-CoV-2 compared to mock controls did not lead to a significant increase in lactate dehydrogenase (LDH), a common marker of tissue injury,[34] nor in pro-inflammatory cytokines correlating with COVID-19 severity (Figures 3A and 3B).[35] Increased levels

---

Figure 2. Subcellular localization of SARS-CoV-2 RNA and proteins in infected human placenta PCSs

(A) Representative *in situ* hybridization micrographs of the RNA of SARS-CoV-2 S protein (pink) in cross-sections of placenta PCSs infected with 5×10^5 PFU of SARS-CoV-2. The green arrows indicate S protein RNA+ cells compatible with Hofbauer cell morphology. The sections were counterstained with hematoxylin. Scale bar, 200 μm.

(B) Representative illustrations of mock- and SARS-CoV-2 infected placenta PCSs analyzed 72 and 120 h p.i. DAPI (blue) SARS-CoV-2 N protein (green) and CANX (red). Scale bar, 10 μm.

(C) High-resolution 3-dimensional (3D) stacks. Upper panels: bright-field images showing the microstructure of human placenta villi. The colored squares represent the zoomed area depicted in the lower panels, which are representative illustrations of syncytiotrophoblasts, expressing CANX (red) and SARS-CoV-2 N protein (green). In the lower panel, the white signal indicates SARS-CoV-2 N protein and CANX co-localization. The percentages of SARS-CoV-2 N protein signal co-localizing with CANX signal are indicated (coloc.). Blue scale bar, 10 μm; white scale bar, 2 μm.

(D) Representative illustrations of mock- and SARS-CoV-2-infected placenta PCSs analyzed 24, 72, and 120 h p.i. DAPI (blue) SARS-CoV-2 N protein (green) and ERp57 (red). Scale bar, 5 μm.

(E) Representative illustrations of mock- and SARS-CoV-2-infected placenta PCSs analyzed 24, 72, and 120 h p.i. DAPI (blue) SARS-CoV-2 S protein (green) and ERp57 (red). Scale bar, 20 μm.

of IFN-λs were measured, while not reaching statistical significance (p = 0.10; Figure 3C).

DISCUSSION

In this study, we evaluated the susceptibility of the human placenta to SARS-CoV-2 replication using an advanced *ex vivo* system modeling the human maternal-fetal interface. We show that placenta PCSs preserve the microstructure of the native tissue and can be cultivated up to 1 week following specimen procurement. Furthermore, our data provide evidence that SARS-CoV-2 infection results in a full replication cycle in the placenta, causing infectious virus release, which indicates a possible propagation of the infection to surrounding tissues.

The studies analyzing the expression of ACE2 and TMPRSS2 throughout pregnancy are conflicting. Some indicate a consistent expression throughout gestational stages in humans, and others mention more variable levels, in particular for the TMPRSS2 protease.[6,36–39] In agreement with this, in uninfected tissue, we observed a high donor variability in the expression of both molecules, spanning throughout 3 orders of magnitude. Remarkably, we found a significant association between ACE2 levels and placenta permissiveness to SARS-CoV-2 infection. Concerning the cellular targets of the virus, our data point to the broad cell tropism of SARS-CoV-2. We detected viral RNA and/or viral proteins in several cellular compartments such as syncytiotrophoblasts, trophoblasts, mesenchymal/stromal cells, and possibly Hofbauer macrophages, as previously observed in case reports.[18,40–43]

We detected co-localization of the ER-associated molecules CANX and ERp57 with SARS-CoV-2 N protein. Given that CANX was shown, in the HEK293T cell line, to chaperone coronavirus replication through the maturation of surface glycoproteins, the high co-localization index of CANX and N protein suggests that SARS-CoV-2 may use a similar mechanism in human placenta.[44] Contrary to N protein, we did not detect the S protein in conjunction with the ER marker tested, indicating possibly distinct localization of N and S proteins within the secretory pathway of placenta cells. In agreement with this, the structural proteins S, M, and E are found in different subcellular compartments during the replication of SARS-CoV.[45] Our observations are compatible with the coronavirus life cycle, characterized by a profound rearrangement of ER membranes into a complex replication network of double-vesicle membranes.[46,47] In line with this, a recent study suggests an alteration of the endocytic pathway at the maternal-fetal interface during COVID-19.[48]

The infection of PCSs did not lead to the induction of pro-inflammatory cytokines related to COVID-19 severity,[35] conflicting with a report on pregnant women with COVID-19.[49] Assuming exuberant immune reaction is central to the pathogenesis of COVID-19,[50,51] this discrepancy could be related to the absence of a functional endothelium and immune system in our *ex vivo* system. We detected a trend toward IFN-λs induction in infected placental tissue. Notably, IFN-λs are expressed by trophoblast cells to support placenta function and antiviral defense.[52] In addition, our data are compatible with a paper from Mourad et al.,[53] suggesting that the placental IFN responses to SARS-CoV-2 are related to disease severity.

In summary, we used an advanced *ex vivo* model to study the interaction of SARS-CoV-2 at the human maternal-fetal interface. This system could be used as a translational platform for the screening of antivirals against SARS-CoV-2 and other pathogens potentially targeting the placenta. We demonstrated with independent methods the susceptibility of the human placenta toward SARS-CoV-2 infection with the release of replication-competent virions. These results stress the requirement to perform further work to better evaluate the risks and define the appropriated measures to protect women from adverse pregnancy outcomes related to COVID-19.

Limitations of the study

Considering the lack of a model of COVID-19 during gestation, our experimental approach allows the study of the biology of SARS-CoV-2 in human placenta. However, some limitations should be mentioned. While placenta PCSs are helpful in understanding the initial phases of SARS-CoV-2 infection, it does not constitute an appropriate system for the assessment of the placental barrier and long-term outcomes influenced by immune components. Also, since we used third-trimester placenta, we cannot draw conclusions regarding the replication of SARS-CoV-2 during early pregnancy. However, SARS-CoV-2 RNA has been detected in the placenta during the initial trimesters of pregnancy, indicating that SARS-CoV-2 may also propagate in this tissue during that period.[54,55] It remains unclear how the virus may reach the placental tissue. The RNA of SARS-CoV-2 is commonly detected in the serum or plasma of COVID-19 patients, but there is no information regarding the presence of infectious virus in peripheral blood.[7] In a recent study, it was hypothesized that infected circulating immune cells may deliver SARS-CoV-2 to the highly vascularized placental tissue.[56]

STAR★METHODS

Detailed methods are provided in the online version of this paper and include the following:

- KEY RESOURCES TABLE
- RESOURCE AVAILABILITY
  - Lead contact
  - Materials availability
  - Data and code availability
- EXPERIMENTAL MODEL AND SUBJECT DETAILS
  - Human placenta precision-cut slice cultures
  - Well-differentiated primary nasal epithelial cells
  - Cell lines
  - Viruses
- METHOD DETAILS
  - Virus infection
  - Virus titration
  - RNA isolation and quantitative PCR
  - Cytotoxicity assay
  - *In situ* hybridization
  - Immunofluorescence
- QUANTIFICATION AND STATISTICAL ANALYSIS
  - Colocalization analysis
  - Statistical analysis

REFERENCES

1. Hou, Y.J., Okuda, K., Edwards, C.E., Martinez, D.R., Asakura, T., Dinnon, K.H., 3rd, Kato, T., Lee, R.E., Yount, B.L., Mascenik, T.M., et al. (2020). SARS-CoV-2 Reverse Genetics Reveals a Variable Infection Gradient in the Respiratory Tract. Cell 182, 429–446.e14.

2. Weatherbee, B.A.T., Glover, D.M., and Zernicka-Goetz, M. (2020). Expression of SARS-CoV-2 receptor *ACE2* and the protease *TMPRSS2* suggests susceptibility of the human embryo in the first trimester. Open Biol. 10, 200162.

3. Cui, D., Liu, Y., Jiang, X., Ding, C., Poon, L.C., Wang, H., and Yang, H. (2021). Single-cell RNA expression profiling of SARS-CoV-2-related ACE2 and TMPRSS2 in human trophectoderm and placenta. Ultrasound Obstet. Gynecol. 57, 248–256.

4. Hikmet, F., Méar, L., Edvinsson, Å., Micke, P., Uhlén, M., and Lindskog, C. (2020). The protein expression profile of ACE2 in human tissues. Mol. Syst. Biol. 16, e9610.

5. Li, M., Chen, L., Zhang, J., Xiong, C., and Li, X. (2020). The SARS-CoV-2 receptor ACE2 expression of maternal-fetal interface and fetal organs by single-cell transcriptome study. PLoS ONE 15, e0230295.

6. Gengler, C., Dubruc, E., Favre, G., Greub, G., de Leval, L., and Baud, D. (2021). SARS-CoV-2 ACE-receptor detection in the placenta throughout pregnancy. Clin. Microbiol. Infect. 27, 489–490.

7. Huang, C., Wang, Y., Li, X., Ren, L., Zhao, J., Hu, Y., Zhang, L., Fan, G., Xu, J., Gu, X., et al. (2020). Clinical features of patients infected with 2019 novel coronavirus in Wuhan, China. Lancet 395, 497–506.

8. Ackermann, M., Verleden, S.E., Kuehnel, M., Haverich, A., Welte, T., Laenger, F., Vanstapel, A., Werlein, C., Stark, H., Tzankov, A., et al. (2020). Pulmonary Vascular Endothelialitis, Thrombosis, and Angiogenesis in Covid-19. N. Engl. J. Med. 383, 120–128.

9. Ellington, S., Strid, P., Tong, V.T., Woodworth, K., Galang, R.R., Zambrano, L.D., Nahabedian, J., Anderson, K., and Gilboa, S.M. (2020). Characteristics of Women of Reproductive Age with Laboratory-Confirmed SARS-CoV-2 Infection by Pregnancy Status - United States, January 22-June 7, 2020. MMWR Morb. Mortal. Wkly. Rep. 69, 769–775.

10. Allotey, J., Stallings, E., Bonet, M., Yap, M., Chatterjee, S., Kew, T., Debenham, L., Llavall, A.C., Dixit, A., Zhou, D., et al.; PregCOV-19 Living Systematic Review Consortium (2020). Clinical manifestations, risk factors, and maternal and perinatal outcomes of coronavirus disease 2019 in pregnancy: living systematic review and meta-analysis. BMJ 370, m3320.

11. Villar, J., Ariff, S., Gunier, R.B., Thiruvengadam, R., Rauch, S., Kholin, A., Roggero, P., Prefumo, F., do Vale, M.S., Cardona-Perez, J.A., et al. (2021). Maternal and Neonatal Morbidity and Mortality Among Pregnant Women With and Without COVID-19 Infection: The INTERCOVID Multinational Cohort Study. JAMA Pediatr. 175, 817–826.

12. Zaigham, M., and Andersson, O. (2020). Maternal and perinatal outcomes with COVID-19: a systematic review of 108 pregnancies. Acta Obstet. Gynecol. Scand. 99, 823–829.

13. Liu, Y., Chen, H., Tang, K., and Guo, Y. (2020). Withdrawn: clinical manifestations and outcome of SARS-CoV-2 infection during pregnancy. J. Infect., S0163-4453(20)30109-2.

14. Baud, D., Greub, G., Favre, G., Gengler, C., Jaton, K., Dubruc, E., and Pomar, L. (2020). Second-Trimester Miscarriage in a Pregnant Woman With SARS-CoV-2 Infection. JAMA 323, 2198–2200.

15. Jering, K.S., Claggett, B.L., Cunningham, J.W., Rosenthal, N., Vardeny, O., Greene, M.F., and Solomon, S.D. (2021). Clinical Characteristics and Outcomes of Hospitalized Women Giving Birth With and Without COVID-19. JAMA Intern. Med. 181, 714–717.

16. Di Mascio, D., Khalil, A., Saccone, G., Rizzo, G., Buca, D., Liberati, M., Vecchiet, J., Nappi, L., Scambia, G., Berghella, V., and D'Antonio, F. (2020). Outcome of coronavirus spectrum infections (SARS, MERS, COVID-19) during pregnancy: a systematic review and meta-analysis. Am. J. Obstet. Gynecol. MFM 2, 100107.

17. Schwartz, D.A., Baldewijns, M., Benachi, A., Bugatti, M., Collins, R.R.J., De Luca, D., Facchetti, F., Linn, R.L., Marcelis, L., Morotti, D., et al. (2021). Chronic Histiocytic Intervillositis with Trophoblast Necrosis are Risk Factors Associated with Placental Infection from Coronavirus Disease 2019 (COVID-19) and Intrauterine Maternal-Fetal Severe Acute Respiratory Syndrome Coronavirus 2 (SARS-CoV-2) Transmission in Liveborn and Stillborn Infants. Arch. Pathol. Lab. Med. 145, 517–528.

18. Schwartz, D.A., and Morotti, D. (2020). Placental Pathology of COVID-19 with and without Fetal and Neonatal Infection: Trophoblast Necrosis and Chronic Histiocytic Intervillositis as Risk Factors for Transplacental Transmission of SARS-CoV-2. Viruses 12, E1308.

19. He, M., Skaria, P., Kreutz, K., Chen, L., Hagemann, I.S., Carter, E.B., Mysorekar, I.U., Nelson, D.M., Pfeifer, J., and Dehner, L.P. (2020). Histopathology of Third Trimester Placenta from SARS-CoV-2-Positive Women. Fetal Pediatr. Pathol. https://doi.org/10.1080/15513815.2020.1828517.

20. Hosier, H., Farhadian, S.F., Morotti, R.A., Deshmukh, U., Lu-Culligan, A., Campbell, K.H., Yasumoto, Y., Vogels, C.B., Casanovas-Massana, A., Vijayakumar, P., et al. (2020). SARS-CoV-2 infection of the placenta. J. Clin. Invest. 130, 4947–4953.

21. Penfield, C.A., Brubaker, S.G., Limaye, M.A., Lighter, J., Ratner, A.J., Thomas, K.M., Meyer, J.A., and Roman, A.S. (2020). Detection of severe acute respiratory syndrome coronavirus 2 in placental and fetal membrane samples. Am. J. Obstet. Gynecol. MFM 2, 100133.

22. Roberts, D.J., Edlow, A.G., Romero, R.J., Coyne, C.B., Ting, D.T., Hornick, J.L., Zaki, S.R., Adhikari, U.D., Serghides, L., Gaw, S.L., and Metz, T.D.; National Institutes of Health/Eunice Kennedy Shriver National Institute of Child Health and Human Development SARS-CoV-2 Placental Infection Workshop (2021). A standardized definition of placental infection by SARS-CoV-2, a consensus statement from the National Institutes of Health/Eunice Kennedy Shriver National Institute of Child Health and Human Development SARS-CoV-2 Placental Infection Workshop. Am. J. Obstet. Gynecol., S0002-9378(21)00832-2.

23. Kotlyar, A.M., Grechukhina, O., Chen, A., Popkhadze, S., Grimshaw, A., Tal, O., Taylor, H.S., and Tal, R. (2021). Vertical transmission of coronavirus disease 2019: a systematic review and meta-analysis. Am. J. Obstet. Gynecol. 224, 35–53.e3.

24. Vivanti, A.J., Vauloup-Fellous, C., Prevot, S., Zupan, V., Suffee, C., Do Cao, J., Benachi, A., and De Luca, D. (2020). Transplacental transmission of SARS-CoV-2 infection. Nat. Commun. 11, 3572.

25. Masmejan, S., Pomar, L., Favre, G., Panchaud, A., Giannoni, E., Greub, G., and Baud, D. (2020). Vertical transmission and materno-fetal outcomes in 13 patients with coronavirus disease 2019. Clin. Microbiol. Infect. 26, 1585–1587.

26. Raschetti, R., Vivanti, A.J., Vauloup-Fellous, C., Loi, B., Benachi, A., and De Luca, D. (2020). Synthesis and systematic review of reported neonatal SARS-CoV-2 infections. Nat. Commun. *11*, 5164.

27. Shamir, E.R., and Ewald, A.J. (2014). Three-dimensional organotypic culture: experimental models of mammalian biology and disease. Nat. Rev. Mol. Cell Biol. *15*, 647–664.

28. Marzioni, D., Mühlhauser, J., Crescimanno, C., Banita, M., Pierleoni, C., and Castellucci, M. (1998). BCL-2 expression in the human placenta and its correlation with fibrin deposits. Hum. Reprod. *13*, 1717–1722.

29. Lipinski, M., Parks, D.R., Rouse, R.V., and Herzenberg, L.A. (1981). Human trophoblast cell-surface antigens defined by monoclonal antibodies. Proc. Natl. Acad. Sci. USA *78*, 5147–5150.

30. Verheije, M.H., Hagemeijer, M.C., Ulasli, M., Reggiori, F., Rottier, P.J., Masters, P.S., and de Haan, C.A. (2010). The coronavirus nucleocapsid protein is dynamically associated with the replication-transcription complexes. J. Virol. *84*, 11575–11579.

31. V'Kovski, P., Kratzel, A., Steiner, S., Stalder, H., and Thiel, V. (2021). Coronavirus biology and replication: implications for SARS-CoV-2. Nat. Rev. Microbiol. *19*, 155–170.

32. Pieren, M., Galli, C., Denzel, A., and Molinari, M. (2005). The use of calnexin and calreticulin by cellular and viral glycoproteins. J. Biol. Chem. *280*, 28265–28271.

33. Ellgaard, L., and Ruddock, L.W. (2005). The human protein disulphide isomerase family: substrate interactions and functional properties. EMBO Rep. *6*, 28–32, 10.

34. Glick, J.H., Jr. (1969). Serum lactate dehydrogenase isoenzyme and total lactate dehydrogenase values in health and disease, and clinical evaluation of these tests by means of discriminant analysis. Am. J. Clin. Pathol. *52*, 320–328.

35. Del Valle, D.M., Kim-Schulze, S., Huang, H.H., Beckmann, N.D., Nirenberg, S., Wang, B., Lavin, Y., Swartz, T.H., Madduri, D., Stock, A., et al. (2020). An inflammatory cytokine signature predicts COVID-19 severity and survival. Nat. Med. *26*, 1636–1643.

36. Faure-Bardon, V., Isnard, P., Roux, N., Leruez-Ville, M., Molina, T., Bessieres, B., and Ville, Y. (2021). Protein expression of angiotensin-converting enzyme 2, a SARS-CoV-2-specific receptor, in fetal and placental tissues throughout gestation: new insight for perinatal counseling. Ultrasound Obstet. Gynecol. *57*, 242–247.

37. Taglauer, E., Benarroch, Y., Rop, K., Barnett, E., Sabharwal, V., Yarrington, C., and Wachman, E.M. (2020). Consistent localization of SARS-CoV-2 spike glycoprotein and ACE2 over TMPRSS2 predominance in placental villi of 15 COVID-19 positive maternal-fetal dyads. Placenta *100*, 69–74.

38. Colson, A., Depoix, C.L., Dessilly, G., Baldin, P., Danhaive, O., Hubinont, C., Sonveaux, P., and Debiève, F. (2021). Clinical and in Vitro Evidence against Placenta Infection at Term by Severe Acute Respiratory Syndrome Coronavirus 2. Am. J. Pathol. *191*, 1610–1623.

39. Bloise, E., Zhang, J., Nakpu, J., Hamada, H., Dunk, C.E., Li, S., Imperio, G.E., Nadeem, L., Kibschull, M., Lye, P., et al. (2021). Expression of severe acute respiratory syndrome coronavirus 2 cell entry genes, angiotensin-converting enzyme 2 and transmembrane protease serine 2, in the placenta across gestation and at the maternal-fetal interface in pregnancies complicated by preterm birth or preeclampsia. Am. J. Obstet. Gynecol. *224*, 298.e1–298.e8.

40. Morotti, D., Cadamuro, M., Rigoli, E., Sonzogni, A., Gianatti, A., Parolin, C., Patanè, L., and Schwartz, D.A. (2021). Molecular Pathology Analysis of SARS-CoV-2 in Syncytiotrophoblast and Hofbauer Cells in Placenta from a Pregnant Woman and Fetus with COVID-19. Pathogens *10*, 479.

41. Schwartz, D.A., Baldewijns, M., Benachi, A., Bugatti, M., Bulfamante, G., Cheng, K., Collins, R.R.J., Debelenko, L., De Luca, D., Facchetti, F., et al. (2021). Hofbauer Cells and COVID-19 in Pregnancy. Arch. Pathol. Lab. Med. *145*, 1328–1340.

42. Verma, S., Joshi, C.S., Silverstein, R.B., He, M., Carter, E.B., and Mysorekar, I.U. (2021). SARS-CoV-2 colonization of maternal and fetal cells of the human placenta promotes alteration of local renin-angiotensin system. Med (N Y) *2*, 575–590.e5.

43. Ashary, N., Bhide, A., Chakraborty, P., Colaco, S., Mishra, A., Chhabria, K., Jolly, M.K., and Modi, D. (2020). Single-Cell RNA-seq Identifies Cell Subsets in Human Placenta That Highly Expresses Factors Driving Pathogenesis of SARS-CoV-2. Front. Cell Dev. Biol. *8*, 783.

44. Fukushi, M., Yoshinaka, Y., Matsuoka, Y., Hatakeyama, S., Ishizaka, Y., Kirikae, T., Sasazuki, T., and Miyoshi-Akiyama, T. (2012). Monitoring of S protein maturation in the endoplasmic reticulum by calnexin is important for the infectivity of severe acute respiratory syndrome coronavirus. J. Virol. *86*, 11745–11753.

45. Nal, B., Chan, C., Kien, F., Siu, L., Tse, J., Chu, K., Kam, J., Staropoli, I., Crescenzo-Chaigne, B., Escriou, N., et al. (2005). Differential maturation and subcellular localization of severe acute respiratory syndrome coronavirus surface proteins S, M and E. J. Gen. Virol. *86*, 1423–1434.

46. Knoops, K., Kikkert, M., Worm, S.H., Zevenhoven-Dobbe, J.C., van der Meer, Y., Koster, A.J., Mommaas, A.M., and Snijder, E.J. (2008). SARS-coronavirus replication is supported by a reticulovesicular network of modified endoplasmic reticulum. PLoS Biol. *6*, e226.

47. Stertz, S., Reichelt, M., Spiegel, M., Kuri, T., Martínez-Sobrido, L., García-Sastre, A., Weber, F., and Kochs, G. (2007). The intracellular sites of early replication and budding of SARS-coronavirus. Virology *361*, 304–315.

48. Benarroch, Y., Juttukonda, L., Sabharwal, V., Boateng, J., Khan, A.R., Yarrington, C., Wachman, E.M., and Taglauer, E. (2021). Differential Expression of Rab5 and Rab7 Small GTPase Proteins in Placental Tissues From Pregnancies Affected by Maternal Coronavirus Disease 2019. Clin. Ther. *43*, 308–318.

49. Lu-Culligan, A., Chavan, A.R., Vijayakumar, P., Irshaid, L., Courchaine, E.M., Milano, K.M., Tang, Z., Pope, S.D., Song, E., Vogels, C.B.F., et al.; Yale IMPACT Team (2021). Maternal respiratory SARS-CoV-2 infection in pregnancy is associated with a robust inflammatory response at the maternal-fetal interface. Med (N Y) *2*, 591–610.e10.

50. Lowery, S.A., Sariol, A., and Perlman, S. (2021). Innate immune and inflammatory responses to SARS-CoV-2: implications for COVID-19. Cell Host Microbe *29*, 1052–1062.

51. Verma, S., Carter, E.B., and Mysorekar, I.U. (2020). SARS-CoV2 and pregnancy: an invisible enemy? Am. J. Reprod. Immunol. *84*, e13308.

52. Yockey, L.J., Jurado, K.A., Arora, N., Millet, A., Rakib, T., Milano, K.M., Hastings, A.K., Fikrig, E., Kong, Y., Horvath, T.L., et al. (2018). Type I interferons instigate fetal demise after Zika virus infection. Sci. Immunol. *3*, eaao1680.

53. Mourad, M., Jacob, T., Sadovsky, E., Bejerano, S., Simone, G.S., Bagalkot, T.R., Zucker, J., Yin, M.T., Chang, J.Y., Liu, L., et al. (2021). Placental response to maternal SARS-CoV-2 infection. Sci. Rep. *11*, 14390.

54. Valdespino-Vázquez, M.Y., Helguera-Repetto, C.A., León-Juárez, M., Villavicencio-Carrisoza, O., Flores-Pliego, A., Moreno-Verduzco, E.R., Díaz-Pérez, D.L., Villegas-Mota, I., Carrasco-Ramírez, E., López-Martínez, I.E., et al. (2021). Fetal and placental infection with SARS-CoV-2 in early pregnancy. J. Med. Virol. *93*, 4480–4487.

55. Shende, P., Gaikwad, P., Gandhewar, M., Ukey, P., Bhide, A., Patel, V., Bhagat, S., Bhor, V., Mahale, S., Gajbhiye, R., and Modi, D. (2021). Persistence of SARS-CoV-2 in the first trimester placenta leading to transplacental transmission and fetal demise from an asymptomatic mother. Hum. Reprod. *36*, 899–906.

56. Lye, P., Dunk, C.E., Zhang, J., Wei, Y., Nakpu, J., Hamada, H., Imperio, G.E., Bloise, E., Matthews, S.G., and Lye, S.J. (2021). ACE2 Is Expressed in Immune Cells That Infiltrate the Placenta in Infection-Associated Preterm Birth. Cells *10*, 1724.

57. Gilligan, J., Tong, M., Longato, L., de la Monte, S.M., and Gundogan, F. (2012). Precision-cut slice culture method for rat placenta. Placenta *33*, 67–72.

58. Schögler, A., Blank, F., Brügger, M., Beyeler, S., Tschanz, S.A., Regamey, N., Casaulta, C., Geiser, T., and Alves, M.P. (2017). Characterization of pediatric cystic fibrosis airway epithelial cell cultures at the air-liquid interface obtained by non-invasive nasal cytology brush sampling. Respir. Res. *18*, 215.

59. Livak, K.J., and Schmittgen, T.D. (2001). Analysis of relative gene expression data using real-time quantitative PCR and the 2(-Delta Delta C(T)) Method. Methods *25*, 402–408.

60. Gielen, V., Sykes, A., Zhu, J., Chan, B., Macintyre, J., Regamey, N., Kieninger, E., Gupta, A., Shoemark, A., Bossley, C., et al. (2015). Increased nuclear suppressor of cytokine signaling 1 in asthmatic bronchial epithelium suppresses rhinovirus induction of innate interferons. J. Allergy Clin. Immunol. *136*, 177–188.e11.

61. Slater, L., Bartlett, N.W., Haas, J.J., Zhu, J., Message, S.D., Walton, R.P., Sykes, A., Dahdaleh, S., Clarke, D.L., Belvisi, M.G., et al. (2010). Co-ordinated role of TLR3, RIG-I and MDA5 in the innate response to rhinovirus in bronchial epithelium. PLoS Pathog. *6*, e1001178.

62. Corman, V.M., Landt, O., Kaiser, M., Molenkamp, R., Meijer, A., Chu, D.K., Bleicker, T., Brünink, S., Schneider, J., Schmidt, M.L., et al. (2020). Detection of 2019 novel coronavirus (2019-nCoV) by real-time RT-PCR. Euro Surveill. *25*, 2000045.

63. Millward-Sadler, S.J., Costello, P.W., Freemont, A.J., and Hoyland, J.A. (2009). Regulation of catabolic gene expression in normal and degenerate human intervertebral disc cells: implications for the pathogenesis of intervertebral disc degeneration. Arthritis Res. Ther. *11*, R65.

64. Contoli, M., Message, S.D., Laza-Stanca, V., Edwards, M.R., Wark, P.A., Bartlett, N.W., Kebadze, T., Mallia, P., Stanciu, L.A., Parker, H.L., et al. (2006). Role of deficient type III interferon-lambda production in asthma exacerbations. Nat. Med. *12*, 1023–1026.

STAR★METHODS

KEY RESOURCES TABLE

REAGENT or RESOURCE	SOURCE	IDENTIFIER
Antibodies		
TROP2 Goat anti-Human, polyclonal	Fisher Scientific	Cat#PA547030; RRID: AB_2609571
SARS/SARS-CoV-2 Nucleocapsid monoclonal antibody	Fisher Scientific	E16C, Cat#MA17403; RRID: AB_1018420
SARS/SARS-CoV-2 Spike S1 monoclonal antibody	Fisher Scientific	GT263, Cat#MA536245; RRID: AB_2890584
ERp57, Goat anti-Human, polyclonal	Abcam	Cat#Ab13507; RRID: AB_300410
Bcl-2, Mouse anti-Human, monoclonal antibody	Bio-Rad	Cat#MCA1550; RRID: AB_2064303
Calnexin Rabbit anti-human, polyclonal	Enzo Life Sciences	Cat#ADI-SPA-860-F; RRID: AB_11178981
Goat anti-IgG Rabbit, AF546, polyclonal	Fisher Scientific	Cat#A11035; RRID: AB_2534093
Goat anti-mouse IgG2a-AF488	Fisher Scientific	Cat#A21131; RRID: AB_2535771
Bacterial and virus strains		
SARS-CoV-2	Kindly provided by Dr. Daniela Niemeyer, PD Dr. Marcel Müller and Prof. Dr. Christian Drosten	SARS-CoV-2/München1.1/2020/929
Biological samples		
Human term placenta	Materno-Fetal and Obstetrics Research Unit, Department University Hospital, Lausanne, Switzerland	N/A
Primary human nasal epithelial cells	Epithelix Sàrl	Cat#EP40AB
Chemicals, peptides, and recombinant proteins		
PBS	GIBCO	Cat#14200067
Agarose, Low melting point	Promega	Cat#V2111
Penicillin/Streptomycin	GIBCO	Cat#15140-122
DMEM GlutaMax	GIBCO	Cat#32430-027
Fetal bovine serum	GIBCO	Cat#10270
HEPES	GIBCO	Cat#15630-056
Glutamine	GIBCO	Cat#35050-038
MEM-NEAA	GIBCO	Cat#11140-035
Avicel RC-581NF	IMCD	N/A
Formalin 4%	Formafix	2011130
Ethanol	Merck	Cat#1.00588.2511
Xylene	Sigma-Aldrich	Cat#102398932
Ammonium chloride	Merck	Cat#1.01145.1000
Citrate	Merck	Cat#441246344
Saponin	Applichem	Cat#A4518
Collagen solution from calf skin	Sigma	Cat#C8919
PneumaCult – Ex Plus Basal Medium	Stem Cell Technologies	Cat#05041
PneumaCult – Ex Plus 50X Supplement	Stem Cell Technologies	Cat#05042
A-83-01	Tocris	Cat#2939
Isoproterenol	Abcam	Cat#ab146724
Hydrocortisone	Stem Cell Technologies	Cat#07925

(Continued on next page)

Continued

REAGENT or RESOURCE	SOURCE	IDENTIFIER
Primocin	InvivoGen	Cat#ant-pm-2
Y-27632	Stem Cell Technologies	Cat#72304
CryoStor CS10	Stem Cell Technologies	Cat#07930
HBSS	GIBCO	Cat#14175-053
PneumaCult - ALI Basal Medium	Stem Cell Technologies	Cat#05002
PneumaCult- ALI 10X Supplement	Stem Cell Technologies	Cat#05003
PneumaCult- ALI Maintenance Supplement 100X	Stem Cell Technologies	Cat#05006
Heparin Solution 0,2%	Stem Cell Technologies	Cat#07980
Crystal violet powder	Sigma	Cat#61135
Hematoxylin	Roth	Cat#89471
VectaMount	Bio-Techne	Cat#321584
Mowiol	Merck	Cat#475904-100
DAPI	Sigma	Cat#D9542
Critical commercial assays		
Nucleospin RNA Plus Kit	Macherey-Nagel	Cat#740984
Omniscript RT Kit	QIAGEN	Cat#52906
CytoTox 96 Non-Radioactive Cytotoxicity Assay	Promega	Cat#G1781
RNAscope technology Kit	Bio-Techne	Cat#300110
TaqMan Fast Universal PCR Master Mix (2x), no AmpErase UNG	Fisher Scientific	Cat#4352042
Experimental models: Cell lines		
Vero E6	Kindly provided by Dr. Doreen Muth, Dr. Marcel Müller, Dr. Christian Drosten	N/A
MDCK	Kindly provided by Dr. Gert Zimmer	
Oligonucleotides		
Hs01085333_m1 (ACE2): FAM-MGB	Fisher Scientific	Cat#4331182
Hs01122322_m1 (TMPRSS2): FAM-MGB	Fisher Scientific	Cat#4331182
18S rRNA (M10098) Forward Primer	Microsyth[57]	5′- CGCCGCTAGAGGTGAAATTCT-3′
18S rRNA (M10098) Reverse Primer	Microsynth AG	5′-CATTCTTGGCAAATGCTTTCG-3′
18S rRNA (M10098) Probe: FAM-TAMRA	Microsynth AG	5′-ACCGGCGCAAGACGGACCAGA-3′
E Sarbeco Forward Primer	Microsynth AG	5′-ACAGGTACGTTAATAGTTAATAGCGT-3′
E Sarbeco Reverse Primer	Microsynth AG	5′-ATATTGCAGCAGTACGCACACA-3′
E Sarbeco P1 Probe: FAM-BBQ	Microsynth AG	5′-ACACTAGCCATCCTTACTGCGCTTCG-3′
IL-6 Forward Primer	Microsynth AG	5′-CCAGGAGCCCAGCTATGAAC-3′
IL-6 Reverse Primer	Microsynth AG	5′-CCCAGGGAGAAGGCAACTG-3′
IL-6 Probe: FAM-TAMRA	Microsynth AG	5′-CCTTCTCCACAAGCGCCTTCGGT-3′
TNF (NM_000594) Forward Primer	Microsynth AG	5′-CGAACATCCAACCTTCCCAAAC-3′
TNF (NM_000594) Reverse Primer	Microsynth AG	5′-TGGTGGTCTTGTTGCTTAAAGTTC-3′
TNF (NM_000594) Probe: FAM-BHQ1	Microsynth AG	5′-CCAATCCCTTTATTACCC-3′
IP-10 (NM_001565) Forward Primer	Microsynth AG	5′-CCATTCTGATTTGCTGCCTTATC-3′
IP-10 (NM_001565) Reverse Primer	Microsynth AG	5′-GCAGGTACAGCGTACAGTTCT-3′
IP-10 (NM_001565) Probe: FAM-TAMRA	Microsynth AG	5′-CTGACTCTAAGTGGCATTCAAGGAGTACCTCTCTC-3′
IFN-β Forward Primer	Microsynth AG	5′-CGCCGCATTGACCATCTA-3′
IFN-β Reverse Primer	Microsynth AG	5′-TTAGCCAGGAGGTTCTCAACAATAGTGTCA-3′
IFN-β Probe: FAM-BHQ1	Microsynth AG	5′-TCAGACAAGATTCATCTAGCACTGGCTGGA-3′

(Continued on next page)

Continued

REAGENT or RESOURCE	SOURCE	IDENTIFIER
IFN-λ1 Forward Primer	Microsynth AG	5′-GGACGCCTTGGAAGAGTCACT-3′
IFN-λ1 Reverse Primer	Microsynth AG	5′-AGAAGCCTCAGGTCCCAATTC-3′
IFN-λ1 Probe: FAM-BHQ1	Microsynth AG	5′-AGTTGCAGCTCTCCTGTCTTCCCCG-3′
IFN- λ2/3 Forward Primer	Microsynth AG	5′-CTGCCACATAGCCCAGTTCA-3′
IFN- λ2/3 Reverse Primer	Microsynth AG	5′-AGAAGCGACTCTTCTAAGGCATCTT-3′
IFN- λ2/3 Probe: FAM-BHQ1	Microsynth AG	5′-TCTCCACAGGAGCTGCAGGCCTTTA-3′
Random hexamer primers	Fisher Scientific	Cat#58875
SARS-CoV2 target probes	ACD Bio-Techne	Cat#V-nCoV20 19-S
Software and algorithms		
IMARIS 9.2.0 software	Bitplane AG	N/A
Prism 9 software	GraphPad	N/A
SDS software v1.4	Applied Biosystems	N/A
Other		
VT1200/S vibrating-blade microtome	Leica Microsystems	N/A
Volt/Ohm Meter, EVOM^2/STX2	World Precision Instruments	EVOM^2
ABI Fast 7500 Sequence Detection System	Applied Biosystems	N/A
Leica RM2135 microtome	Leica Biosystems	N/A
HybEZTM Oven	ACD Bio-Techne	Cat#PN 321710/321720
Nikon Eclipse Ci-L microscope	Nikon Instruments Europe BV	N/A
DS-FI3 camera	Nikon Instruments Europe BV	N/A
Nikon Eclipse Ti	Nikon Instruments Europe BV	N/A
Carl Zeiss LSM 710	Carl Zeiss AG, Feldbach, Switzerland	N/A
Biotek 800 TS absorbance reader	Agilent technologies	N/A

RESOURCE AVAILABILITY

Lead contact
Further information and requests for resources and reagents should be directed to and will be fulfilled by the lead contact, Marco P. Alves (marco.alves@vetsuisse.unibe.ch).

Materials availability
All unique/stable reagents generated in this study are available from the lead contact with a completed Materials Transfer Agreement.

Data and code availability
This study does not report original computer codes or algorithms. The data generated and analyzed during the current study are available from the lead contact upon request.

EXPERIMENTAL MODEL AND SUBJECT DETAILS

Human placenta precision-cut slice cultures
The placenta specimens were obtained from patients tested negative for SARS-CoV-2 by PCR 24 h before undergoing elective C-section (donors 1-3, 5, and 7) or vaginal delivery (donors 4 and 6) at term pregnancy (> 37 weeks of gestation). C-sections were performed for breech position of the babies, maternal request or previous C-section. Furthermore, the patients selected had all uneventful pregnancies and babies had all normal weight and adapted well after birth. Written informed consent was obtained from all the patients and the study protocol agrees with the local Ethics Committee of the Canton of Vaud, Switzerland. The placenta biopsies were about 1-2 cm^2 pieces of placenta taken between the umbilical cord implantation and the margin of the placenta. Each piece included the full thickness of the placenta with both maternal and fetal sides (i.e., membranes). Next, the biopsies were stored in

phosphate buffer solution (PBS, GIBCO) containing 100 units/ml of penicillin and 100 μg/ml streptomycin (all from GIBCO) on ice and transported to the laboratory within 2-3 h. Prior slicing, the biopsies were carefully rinsed with cold PBS and cut at a size of about one cm^3. Human placenta pieces were embedded into 1% of low melting point agarose (Promega) in Peel-A-Way molds S-22 (Sigma) and kept on ice. Sections of 500-700 μm were obtained using a VT1200/S vibrating-blade microtome (Leica Microsystems) with the following settings: speed 0.12-0.26 mm/s, amplitude 3 mm, angle 18°. The human placenta slices were transferred to 6 well plates (TPP) containing 3 mL per well of DMEM GlutaMax (GIBCO), 10% fetal bovine serum (FBS, GIBCO), 10 mM HEPES (GIBCO), 1% Glutamine, 1% MEM-NEAA, 100 units/ml of penicillin and 100 μg/ml streptomycin. To limit the effect of injury caused by the tissue slicing, cultures were maintained at 37°C, 5% CO$_2$ and medium was changed every 24 h for two days prior infection.[57]

Well-differentiated primary nasal epithelial cells

Primary human NECs were obtained commercially (Epithelix Sàrl). The generation of WD-NECs was done as described previously with some adjustments.[58] First, NECs were expanded in collagen-coated (Sigma) cell culture flasks (Costar) in PneumaCult Ex Plus medium, supplemented with 1 μM hydrocortisone, 5 μM Y-27632 (Stem Cell Technologies), 1 μM A-83-01 (Tocris), 3 μM isoproterenol (abcam), and 100 μg/ml primocin (Invivogen), maintained in a humidified incubator at 37°C, 5% CO$_2$, and cryopreserved at −150°C (CryoStor, Stem Cell Technologies). Next, the cryopreserved cells were washed and seeded at a density of 50'000 cells per insert onto collagen-coated (Sigma) onto 24-well plate inserts with a pore size of 0.4 μm (Greiner Bio-One). Cells were grown on the insert membranes under submerged conditions by adding 200 μl complemented PneumaCult ExPlus medium apically and 500 μl in the basolateral chamber until they reached confluence as assessed by measuring the trans-epithelial electrical resistance (TEER) using a Volt/Ohm Meter (EVOM^2/STX2, World Precision Instruments) or microscopical evaluation. Then, apical medium was removed, cells were washed with warm Hank's balanced salt solution (HBSS, GIBCO) prior to exposure to air, and completed PneumaCult ALI medium, supplemented with 4 μg/ml heparin (Stem Cell Technologies), 5 μM hydrocortisone, and 100 μg/ml primocin was added to the basolateral medium to induce differentiation of the cells. The basal medium was changed every 2-3 days and cultures were maintained at 37°C, 5% CO$_2$ until the appearance of ciliated cells and mucus production. To get rid of mucus, the cell layer was washed once a week with pre-warmed 250 μL of pre-warmed HBSS during 20 min at 37°C.

Cell lines

Vero E6 cells were kindly provided by Doreen Muth, Marcel Müller, and Christian Drosten (Charité, Berlin, Germany) and maintained in DMEM GlutaMax supplemented with 10% FBS and 1% HEPES at 37°C, 5% CO2.

Viruses

SARS-CoV-2 (SARS-CoV-2/München1.1/2020/929) isolate passaged once in Vero E6 was kindly provided by Daniela Niemeyer, Marcel Müller, and Christian Drosten from Charité, Berlin, Germany. Next, SARS-CoV-2 was propagated once in Vero E6 cells at a MOI of 0.01 PFU per cell to produce the working stock. Therefore, original isolate was added to the cells in DMEM GlutaMax supplemented with 10% FBS. Supernatant was harvested after 36 h of incubation at 37°C, 5% CO$_2$, centrifuged in order to get rid of cell debris, and then stored in aliquots at −70°C. All the work involving manipulation of SARS-CoV-2 was performed under biosafety level 3 (BSL3) conditions at the Institute of Virology and Immunology, Bern, Switzerland and was authorized by the Federal authorities (authorization no. A202819). Entry into the BSL3 laboratory is only possible following an advanced training and with appropriate personal protective equipment, including a Tyvek overall and hood (both 3M), and a Jupiter air respirator equipped with an HEPA filter system (3M).

METHOD DETAILS

Virus infection

The infection of placenta PCSs with SARS-CoV-2 was performed by applying the inoculum at a rate of 5x10^5 PFU per PCS during 4-6 h at 37°C and 5% CO$_2$, followed by two times wash with pre-warmed PBS. As control, the culture supernatant of mock-infected Vero E6 cells was used. Over the course of infection, supernatants and tissue samples were harvested at selected time points and stored at −80°C until further analysis. Placenta PCSs were fixed in 4% formalin (Formafix) for 24 h for subsequent analysis. For infection of WD-NECs, the virus inoculum was applied apically at a rate of 5x10^4 PFU per insert (representing a MOI of ca. 0.1 PFU per cell) during 2-3 h at 37°C and 5% CO$_2$, followed by three times wash with pre-warmed PBS. As control, the culture supernatant of mock-infected Vero E6 cells was used. For quantification of infectious viral particle release 2, 24, 48, and 72 h p.i., 250 μL of PBS were applied to the apical surface and incubated for 20 min at 37°C, harvested, and stored at −70°C until further analysis.

Virus titration

For virus titration, serial dilutions of supernatants, starting at a 1:2 dilution, were added to Vero E6 cells in a 6-well format. Briefly, 3 x 10^6 cells per plate were seeded 24 h prior the addition of the inoculum. Following 1 h of incubation, cells were overlaid with 2.4% Avicel RC-581NF (IMCD) mixed at 1:1 with DMEM supplemented with 20% FBS, 2x HEPES, 200 units/ml penicillin, and 200 μg/ml streptomycin and kept at 37°C, 5% CO$_2$. After 48 h, the overlay was aspirated, cells were fixed in 4% formalin for 15 min and stained with crystal violet for 10 min. Virus titers were calculated as PFU per ml.

RNA isolation and quantitative PCR

Total RNA of placenta PCSs was extracted using the Nucleospin RNA Plus Kit (Macherey-Nagel) according to the manufacturer's protocol. Next, the Omniscript RT Kit (QIAGEN) using random hexamers (Invitrogen) was applied for reverse transcription and synthesis of complementary DNA (cDNA). On an ABI Fast 7500 Sequence Detection System (Applied Biosystems) qPCR was performed with target-specific primers using the TaqMan Gene Expression Assay (Applied Biosystems). Resulting data were analyzed using the SDS software (Applied Biosystems). Relative expression was calculated with the ΔΔCT method as described.[59] For the analysis of the genes of interest, expression levels were normalized to the housekeeping 18S rRNA. The sequences of the primers and probes used are listed in the key resources table.[60,61–64]

Cytotoxicity assay

Levels of lactate dehydrogenase (LDH) release were assessed in the supernatants of SARS-CoV-2- and mock-infected placenta PCSs using the CytoTox 96 Non-Radioactive Cytotoxicity Assay (Promega) following manufacturer's instructions. Absorbance of four technical replicates per sample was measured at 490 nm with the Biotek 800 TS absorbance reader (Agilent technologies). The percentage of cytotoxicity was calculated by subtracting the culture medium background. Next, the resulting values were divided by the maximum LDH release, which was obtained by incubating adherent Madin-Darby Canine Kidney (MDCK) cells (Kindly provided by Dr. Gert Zimmer, Institute of Virology and Immunology, Switzerland) with 1X lysis solution (provided by the manufacturer) for 30 min.

In situ hybridization

Human placenta PCSs with or without SARS-CoV-2 infection were fixed in 4% formalin (Formafix) overnight and were embedded with paraffin using standard protocol done by the COMparative PATHology platform (COMPATH), Institute of Pathology and Institute of Animal Pathology, University of Bern, Switzerland. In brief, human placenta PCSs were transferred into embedding cassettes and properly labeled. The embedding cassettes were dehydrated using a series of increasing concentration of Ethanol (70%, 96% to 100%; Grogg). As a final step of dehydration, embedding cassettes were transferred to Xylol (Sigma-Aldrich). Next, embedding cassettes were transferred to the beaker containing melted paraffin for 45 min. Paraffin blocks were obtained using a tissue embedding machine. Then, 5 μm thick sections were cut using a Leica RM2135 microtome (Leica Biosystems). Next, the formalin-fixed paraffin-embedded (FFPE) sections were mounted on glass slides (Fisherbrand Superfrost Plus; Fisher Scientific). FFPE sections were dewaxed at 60°C for 1 h followed by standard procedure for rehydration with Xylol and a series of decreasing concentration of Ethanol (100%, 95%, 80% to 70%). *In situ* hybridization of SARS-CoV-2 RNA was done using the RNAscope technology according to manufacturers' instructions (ACD Bio-Techne). The dewaxed sections were treated with RNAscope hydrogene peroxide for 10 min at room temperature. After washing steps in distilled water, the slides were heated with RNAscope Target Retrieval Reagent at 99°C for 15 min. After rinsing with distilled water, slides were put in 100% ethanol for 3 min. After dry out, drops of RNAscope Protease Plus Reagent were added until full coverage of the section. During the whole assay, slides were put on the HybEZTM Slide Rack (ACD Bio-Techne), and incubation steps occurred in the HybEZTM Oven (ACD Bio-Techne). Finally, hybridization was performed using SARS-CoV-2 target probes (V-nCoV20 19-S, ACD Bio-Techne) at 40°C for 2 h. Then, slides went through amplification cycles, following manufacturer's instructions using RNAscope 2.5 HD Detection Reagent-RED Kit. After each amplification step, slides were washed in RNAscope Wash buffer Reagent. Hybridization signals were detected with Fast RED (Advanced Cell Diagnostics), followed by counterstaining with hematoxylin (Roth). Finally, slides were mounted with VectaMount (Advanced Cell Diagnostics). Stained slides were visualized using the upright Nikon Eclipse Ci-L microscope (Nikon Instruments Europe BV). Images were taken using a DS-FI3 camera (Nikon Instruments Europe BV).

Immunofluorescence

Human placenta PCSs were fixed in 4% formalin (Formafix) overnight and were embedded in paraffin using the standard protocol described in the previous section. Then, 5 μm thick sections were cut with a Leica RM2135 microtome (Leica Biosystems). Briefly, sections went through dewaxing with Xylol and rehydration with a series of decreased Ethanol concentrations (100%, 95%, 80% and 70%). After performance of epitope unmasking with 10 mM citrate buffer (Merck), we treated the sections with staining buffer (50 mM ammonium chloride (Merck), 1% FBS (GIBCO), 0.1% saponin (Applichem) in PBS) for 1 h at room temperature. For labeling we used antibodies against SARS-CoV-2 N protein (clone E16C, dilution 1:25, Fisher Scientific), SARS-CoV-2 S protein (clone GT263, dilution 1:25, Fisher Scientific), TROP-2 (polyclonal, dilution 1:50, Fisher Scientific), BCL-2 (clone 100, dilution 1:100, BioRad), Erp57 (polyclonal, dilution 1:50, Abcam), and CANX (polyclonal, dilution 1:200, Enzo Life Sciences). Primary antibodies were incubated at 4°C overnight in a humidified chamber. After a washing step with staining buffer, sections were incubated with secondary antibodies for 1 h at room temperature including anti-mouse IgG-AF488 and anti-rabbit IgG-AF546 (both from Fisher Scientific) and during this step, nuclei were stained with DAPI (Sigma). Slides were mounted with Mowiol (Merck/Calbiochem) and analyzed by confocal microscopy (Nikon Eclipse Ti or Carl Zeiss LSM 710) at the microscopy imaging center (MIC) of the University of Bern, Switzerland. Optical sections were taken with a Zeiss LSM710 (Carl Zeiss AG, Feldbach, Switzerland) confocal microscope. 2D images were acquired using a 40X objective with settings for high-resolution images acquired at optimum voxel size and automatic threshold. 3D images were acquired using a 60X oil-immersion objective. For co-localization analysis, high-resolution images acquired at optimum voxel size were used, automatic threshold applied, and percentage material co-localized were calculated. The images were analyzed using IMARIS

9.2.0 software (Bitplane AG). To eliminate any false-positive emission, all microscopy analyses employed threshold subtraction and gamma-correction, relating to the mock controls.

QUANTIFICATION AND STATISTICAL ANALYSIS

Colocalization analysis

For co-localization analysis, high-resolution stacks acquired at optimum voxel size were used and automatic threshold applied. We selected regions of interest (ROIs), namely CANX-positive regions of placenta PCSs where the presence of SARS-CoV-2-positive structures were noticed. To calculate the percentage of co-localized voxels in the channels under investigation (SARS-CoV-2 N protein signal co-localizing with CANX), the co-localization algorithm of IMARIS 9.2.0 software (Bitplane AG) was applied.

Statistical analysis

The Prism 9 software (GraphPad) was used for statistical analysis. To determine differences between two groups, two-sided t test was used. Associations were tested using the Spearman rank correlation test. A $p < 0.05$ was considered statistically significant.